ACADEMIC PRESS

Available online at www.sciencedirect.com

SCIENCE DIRECT®

Journal of Structural Biology 140 (2002) 92–99

Journal of Structural Biology

www.academicpress.com

Quantitation of GFP-fusion proteins in single living cells

Miroslav Dundr,[a] James G. McNally,[a] Jean Cohen,[b] and Tom Misteli[a,*]

[a] *National Cancer Institute, NIH, 41 Library Drive, Bldg. 41, Bethesda, MD 20892-5055, USA*
[b] *UMR CNRS–INRA Virologie Moleculaire et Structurale, 1 Av. De la Terrasse, Gif-sur-Yvette, France*

Received 25 June 2002, and in revised form 29 August 2002

Abstract

The green fluorescent protein (GFP) has revolutionized cell biology. The ability to observe genetically encoded fluorescently tagged fusion proteins in intact cells has made virtually any biological process amenable to investigation in living cells. However, most in vivo imaging studies are qualitative and little information about the number of fluorescently labeled molecules observed in a cell or a cellular structure is available. This deficiency severely limits the interpretation of imaging experiments and it impedes the application of in vivo imaging methods for biophysical purposes. Here we describe a simple method for the quantitative determination of the number of GFP-tagged molecules in cellular structures in single living cells. The method is based on the use of rotavirus-like particles containing a known number of GFP molecules as an internal calibration standard during in vivo imaging. We have applied this method to estimate in single living cells the number of fluorescent transcription factor molecules on RNA polymerase I and polymerase II genes. In addition, we have estimated the number of molecules for several proteins in subnuclear compartments and in exocytic vesicles. VLP–GFP calibration is a simple, convenient, rapid, and noninvasive method for routine quantification of GFP-labeled molecules in single, living cells.

Keywords: GFP; Quantitation; Microscopy; Nucleolus; RNA polymerase I and II; VLP

1. Introduction

Fluorescence microscopy is widely used for the qualitative determination of protein distributions in fixed and living cells and organisms. The discovery and subsequent optimization of green fluorescence protein isolated from jellyfish *Aequorea victoria* as a genetically encoded fluorescent reporter protein have changed the way we study protein localization in cells. The expression of proteins tagged with GFP in living cells allows to determine not only protein location within the cell over the time but also its mobility and interactions (Chalfie et al., 1994; Phair and Misteli, 2001; van Roessel and Brand, 2002). While fluorescence signals accurately report the relative concentration of a fluorophore, quantitative measurements of the absolute number of fluorescence molecules in cellular structures have been difficult and often impractical. Quantitation is hampered by the requirement for fluorescence calibration standards, which must contain a fixed number of fluorescent groups and which ideally can be imaged in the same sample and under identical imaging conditions as the sample of interest. Such calibration standards are not readily available.

Several methods for the calibration of GFP signals have been reported, but no calibration standard that can directly be used in living samples is currently available. Hirschberg et al. (1998) estimated the number of molecules of vesicular stomatitis virus ts045 G protein fused to GFP expressed in a single cell by comparing the total cellular fluorescent intensity in a defined volumetric region of interest to a standard curve generated with dilution series of known concentrations of recombinant GFP in solution. Chiu et al. (2001) developed a calibration standard using transparent beads (diameter 80–120 nm) with calibrated surface densities of histidine-tagged GFP molecules. By comparison of fluorescence intensities between the calibrated beads in solution and GFP-tagged cationic P2X2 receptors in hippocampal

* Corresponding author. Fax: 1-928-832-0970.
E-mail address: mistelit@mail.nih.gov (T. Misteli).

1047-8477/02/$ - see front matter © 2002 Elsevier Science (USA). All rights reserved.
PII: S1047-8477(02)00521-X

neurons the authors determined the number of GFP receptors per area of neuronal soma (Khakh et al., 2001). Both methods have the advantage that they can be prepared with a wide range of GFP concentrations either in solution or on the surface of the beads to match the fluorescent intensities of a tested sample. However, neither method allows comparison of the calibration signal and test signal in the same sample and under identical imaging conditions. We describe here the use of rotavirus-derived virus-like particles (VLP) as a convenient internal calibration standard for the routine quantitation of GFP proteins in living cells.

Rotavirus is a trilayered virus, which contains the VP2 protein in its innermost layer, the VP6 protein in its medial layer, and the VP7 and VP4 proteins in its outermost layer (Charpilienne et al., 2001; Labbe et al., 1994). The inner layer is made up of 60 asymmetric dimers which are arranged with $T = 1$ icosahedral symmetry and the stoichiometry of coat proteins is strictly maintained among virus particles (Lawton et al., 1997; Prasad et al., 1988). Noninfectious, double-layered virus-like particles can be assembled in a baculovirus expression system by coexpression of VP2 and VP6 (Labbe et al., 1994). When baculovirus assembly is performed in the presence of GFP-tagged VP2 protein, VLPs containing exactly 120 GFP-VP2 molecules in their capsids are assembled, as demonstrated by spectrophotometry and cryo-electron microscopy (Charpilienne et al., 2001). GFP–VLPs appear ideally suited for fluorescence calibration purposes since they contain a known, fixed number of fluorescent groups and they can easily be imaged using fluorescence microscopy (Charpilienne et al., 2001).

2. Materials and methods

2.1. Cell culture and transfection

CMT3 cells were grown to an ~70% confluent monolayer in a 10-cm petri dish in DMEM supplemented with 10% FCS, 1% glutamine, and penicillin and streptomycin at 37 °C in 5% CO_2. Cells were washed with PBS and detached by trypsin, collected by centrifugation at 1000 rpm for 2 min, and resuspended in 200 μl of fresh medium. Next, 30 μl of DNA solution (5 μg plasmid encoding the GFP protein of interest and 15 μg sheared salmon sperm carrier DNA) was added, mixed by pipetting up and down three times, and then transferred to a sterile 2-mm-gap electroporation cuvette, and electroporated in a BTX ECM830 electroporator (150-V, 1-ms pulse, 4 pulses, 0.5-s intervals). Electroporated cells were plated onto 22 × 22-mm glass coverslips and the media were replaced ~6 h after transfection. Mouse 3617 cells were grown as previously described (McNally et al., 2000). 100 nM dexamethasone was added 1 hr prior to observation of 3617 cells containing the MMTV array.

2.2. Microscopy and VLP calibration

Purified GFP–VLP were prepared and purified as described (Charpilienne et al., 2001) and stored as a stock solution of 500 μg/ml. Approximately 16–20 h after transfection, cells on a 22 × 22-mm coverslip were washed twice and floated for 5 min on a drop of ~30–40 μl of 10 μg/ml GFP–VLP at room temperature. Cells were examined on a Zeiss LSM 510 laser scanning confocal microscope using a 100× planapochromat oil objective. The excitation wavelength of the laser was at 488 nm and detection was above 505 nm. The photomultiplier tube sensitivity was adjusted such that the fluorescence signal of the GFP-fusion protein was slightly below the saturation level. Then 12-bit or 16-bit images of cells expressing the GFP-fusion protein were collected. For GFP–VLP calibration single images of the VLP–GFP particles were collected in a different field of view in the same specimen using identical imaging settings. All images were background-subtracted. The average area and the average fluorescence intensity of at least 70 cellular structures of interest containing the GFP-fusion protein and at least 70 GFP–VLP particles were measured in each experiment using Metamorph software (Universal Imaging). The average total fluorescence intensity of GFP–VLPs and of the structure of interest was determined by multiplication of the average area with the average fluorescence intensity. The number of GFP-fusion protein molecules per compartment was calculated as

$$(T_C \times 120)/(T_{VLP}),$$

where T_C is the intensity of the compartment and T_{VLP} is the average total intensity of VLPs measured under identical imaging conditions.

3. Results

We sought to test the usefulness of GFP–VLPs as an in vivo calibration standard for the estimation of GFP signals in living cells. As previously reported, when GFP–VLP particles were imaged using confocal laser scanning microscopy, they appeared as single diffraction-limited spots consistent with their diameter of 50 nm as observed by electron microscopy (Charpilienne et al., 2001) (Fig. 1A). Measurement of the total fluorescence intensities of GFP–VLPs using background subtracted 16-bit images demonstrated that the fluorescence intensity of particles fell within a major peak and that more than 80% of GFP–VLPs fell within a twofold range of intensities with an average of $3.0 \pm 1.2 \times 10^5$ (Fig. 1B). The heterogeneity in fluores-

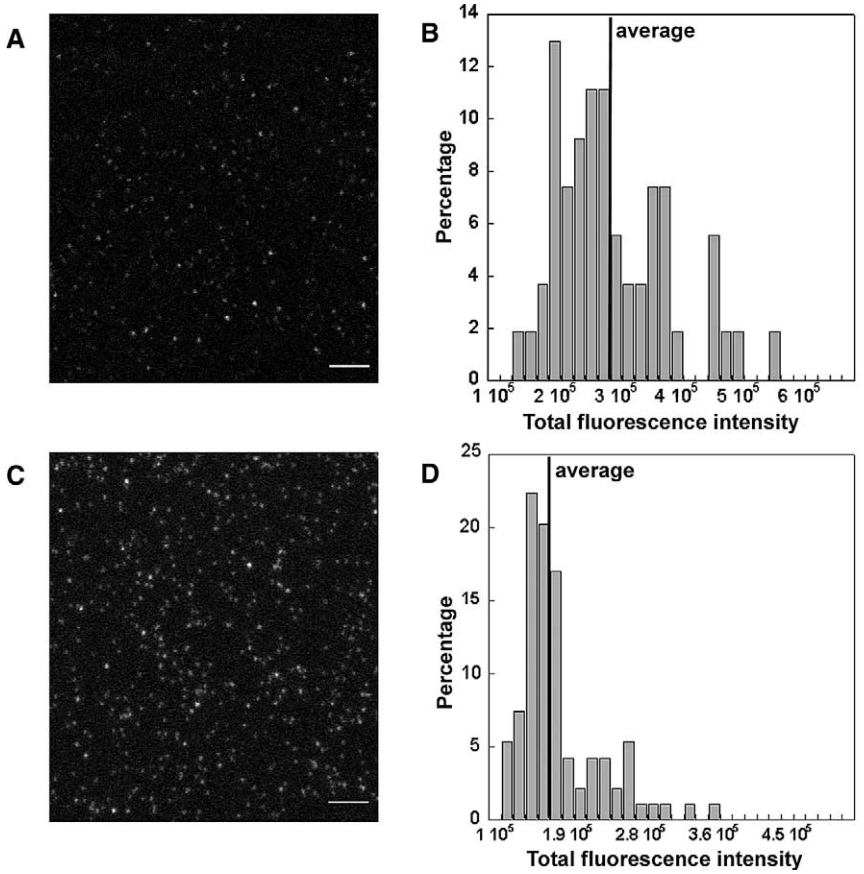

Fig. 1. Visualization of GFP–VLPs by confocal microscopy. (A, C) GFP–VLP particles were visualized by 16-bit laser scanning confocal microscopy in (A) a single optical section or (C) a series of optical sections covering ~400 nm along the optical axis, shown here as an additive projection. (B, D) Histogram of the distribution of the total fluorescence intensity of single particles after background subtraction for (B) a single optical section or (D) an additive projection of the stack. Bars: 3 μm.

cence signals was due to particles partially located outside of the focal plane. When a stack of images covering ~400 nm along the optical axis was acquired and displayed as an additive projection, the GFP–VLP population appeared as a major single peak with an average intensity of $1.8 \pm 0.4 \times 10^5$ (Figs. 1C and D). The GFP–VLP signals increased linearly with increasing PMT gain and the intensity distribution was independent of PMT settings (data not shown). Similar observations were made using 12-bit imaging (data not shown). These observations confirm that GFP–VLPs exist predominantly as single particles, which can be imaged by confocal microscopy.

We tested the suitability of GFP–VLP particles for calibration of fluorescence signals by determining the number of GFP-labeled molecules of the RNA polymerase I subunit RPA40 in the nucleolus of monkey kidney CMT3 cells. The RNA pol I subunit RPA40 is predominantly localized in nucleolar fibrillar centers (FCs), which contain the active ribosomal genes and the active RNA pol I transcription complexes (Olson et al., 2000). This system is ideally suited to test the accuracy of the GFP–VLP calibration method since the number of RPA40 molecules in FCs can be estimated independently of fluorescence measurements. Each FC contains 2–4 active ribosomal genes and each ribosomal gene contains 100–110 active RNA pol I complexes with one RPA40 subunit each (Gilbert et al., 1995; Haaf et al., 1991; Jackson et al., 1993; Paule and White, 2000). Thus, the expected number of RPA40 molecules in a single FC is between 200 and 440 molecules. In order to estimate the number of GFP–RPA40 molecules in a single FC of a living cell using GFP–VLP calibration, we added GFP–VLPs to CMT3 cells expressing GFP–RPA40. Single optical sections of GFP–RPA40 in FCs of single living cells and of GFP–VLPs in the same sample using identical imaging settings were acquired using 12-bit confocal imaging (Figs. 2A and B). Imaging conditions were optimized by adjusting the PMT gain to ensure that the GFP–RPA40 signals were not saturated, but that GFP–VLP were still clearly visible and that both signals were within the linear range of the detector. The total fluorescence intensity of single FCs and the total fluorescence intensity of single GFP–VLPs located in an area devoid of cells was measured in the same sample using identical imaging settings (Figs. 2C and

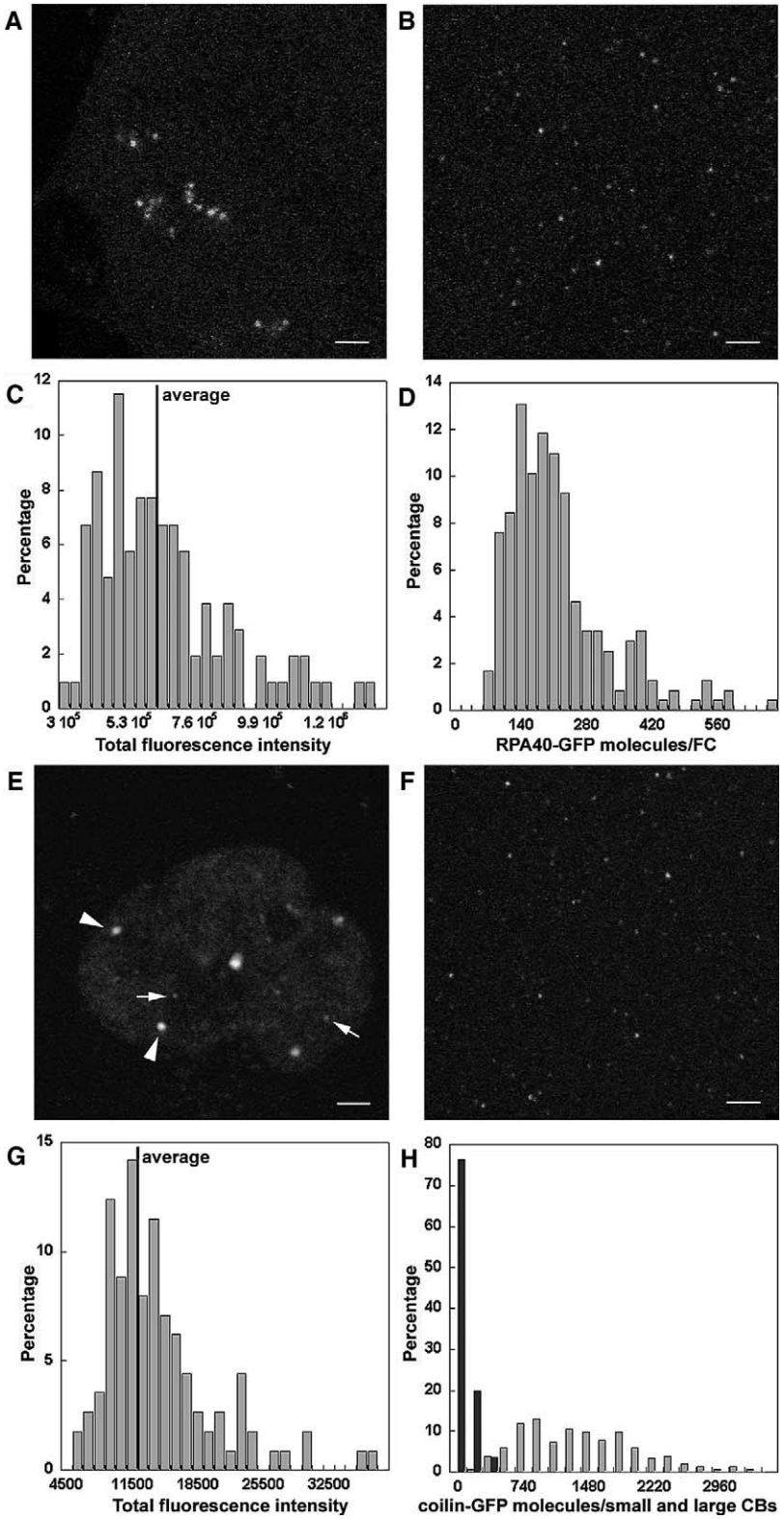

Fig. 2. Determination of the abundance of nuclear proteins. (A) The GFP-tagged RPA40 subunit of RNA polymerase I was transiently expressed in CMT3 cells. GFP–RPA40 accumulated in nucleolar fibrillar centers. (B) GFP–VLPs were visualized in the same specimen using identical imaging settings. (C) Histogram of the distribution of total fluorescence intensity of single VLP particles. (D) Histogram of the distribution of the number of GFP–RPA40 molecules in FCs. (E) GFP-tagged p80-coilin stably expressed in HeLa cells accumulates in large (arrowheads) and small (arrows) Cajal bodies. (F) GFP–VLPs were visualized in the same sample using identical imaging settings. (G) Histogram of the distribution of total fluorescence intensity of single VLP particles. (H) Histogram of the distribution of the number of GFP–p80 coilin molecules in Cajal bodies. Note the presence of two distinct peaks of GFP–p80 coilin numbers corresponding to the two size classes of Cajal bodies. Bars: 2 μm.

D). Under these imaging conditions, GFP–VLP particle intensities were distributed in a predominant peak with an average total intensity of a single GFP–VLP particle of $6.9 \pm 2.6 \times 10^5$ (Fig. 2C). The number of GFP–RPA40 molecules in single FCs could then be calculated as

$$(T_{FC} \times 120)/(T_{VLP}),$$

where T_{FC} is the fluorescence intensity of a single measured FC and T_{VLP} is the average fluorescence intensity of VLP particles under identical imaging conditions. In this manner the average number of GFP–RPA40 subunits in FCs was determined to be 232 ± 117 molecules (Fig. 2D; Table 1). To further confirm the accuracy of GFP–VLP calibration, the abundance of several other components of the RNA polymerase I machinery was analyzed in an analogous manner. We detected between 221 and 410 molecules for each of the GFP-tagged RPA16 and RPA194 subunits of the RNA polymerase I machinery in FCs (Table 1). Like RPA40, each one of these subunits is expected to be present in FCs at 200–600 copies since they form a RNA polymerase I holoenzyme with equimolar stoichiometry (Gilbert et al., 1995; Grummt, 1999; Junera et al., 1997; Paule and White, 2000). For all measured RNA pol I subunits, the number of molecules was within the expected range of 200–440 molecules per FC even when considering a systematic error of about 35% due to the uncertainty of the average intensity for VLP particles (T_{VLP}) caused by the heterogeneity of GFP–VLP particle signals (see Figs. 1B, 2C). Note that the GFP-RPA subunits are overexpressed at least fivefold compared to the endogenous subunits and thus most RNA pol I complexes contain fluorescently tagged subunits. These observations suggest that GFP–VLPs are a suitable calibration standard for the estimation of absolute numbers of GFP molecules in living cells.

We confirmed the suitability of GFP–VLP as a calibration standard in a second experimental system, where the number of expected molecules at a cellular structure can also be estimated independently. We took advantage of a mouse fibroblast cell line stably expressing GFP–glucocorticoid receptor (GFP–GR) and containing an array of 200 mouse mammary tumor virus promoters (MMTV) (McNally et al., 2000). Upon hormone stimulation, GFP–GR translocates from the cytoplasm into the nucleus and associates with the MMTV array where it activates transcription (McNally et al., 2000). Each promoter region contains six GR binding sites and thus the maximal number of GFP–GR molecules bound to the array is 1200. We mixed GFP–VLPs with hormone-stimulated cells expressing GFP–GR, imaged GFP–GR bound to the MMTV array, and compared the fluorescence intensity with GFP–VLP in the same sample using identical imaging conditions. Since the MMTV array often extends beyond a single optical section we imaged both the MMTV array and the VLPs with an open pinhole of 5 Airy units. The average number of GFP–GR molecules on the MMTV array was 722 ± 435 (Table 1). Given that the cell line expresses about five times more GFP–GR (McNally et al., 2000) than endogenous GR it can be estimated that, consistent with the available 1200 binding sites, the MMTV array is on average occupied by 866 ± 501 GR molecules.

We then applied GFP–VLP calibration to estimate the number of molecules of proteins of unknown abundance. Using an approach identical to the one used to determine the number of RNA pol I subunits we estimated that on average each FC contains 308 ± 213 molecules of the GFP-tagged RNA pol I upstream binding factor (UBF1) (Stefanovsky et al., 2001) (Table 1). The somewhat surprisingly high number of GFP–UBF1 molecules in FCs supports the recent observation that UBF does not only anchor the RNA pol I

Table 1
Abundance of GFP-fusion proteins

	Average number of molecules ± SEM	Range
Fibrillar centers		
UBF1–GFP	308 ± 213	104–1779
RPA194–GFP	221 ± 63	110–375
RPA40–GFP	232 ± 117	80–598
RPA16–GFP	410 ± 166	178–974
Cajal body—large		
p80-coilin–GFP	1511 ± 673	399–3289
Fibrillarin–GFP	597 ± 288	204–1332
Cajal body—small		
p80-coilin–GFP	145 ± 92	47–489
MMTV array		
GR–GFP	722 ± 435	420–1254
Exocytic vesicles		
GFP–STAMP1	155 ± 56	65–387

machinery to the 2–4 promoters present within a FC, but also decorates the entire length of ribosomal genes and possibly functions as a structural protein in ribosomal chromatin (O'Sullivan et al., 2002).

In situations where the abundance of a GFP-fusion protein relative to its endogenous counterpart is known, determination of the absolute number of fluorescently tagged molecules allows in theory estimation of total protein abundance. To this end, we took advantage of the existence of a HeLa cell line, which stably expresses GFP–p80-coilin at about 2.5× the level of the endogenous protein as previously demonstrated by Western blotting (Platani et al., 2000). p80-coilin is the major marker protein for Cajal bodies (CBs), a small subnuclear compartment of unknown function (Gall, 2000). Using GFP–VLP we estimated the number of GFP–p80-coilin in CBs of HeLa cells stably expressing GFP–p80-coilin (Figs. 2E and F; Table 1). As observed before, the total fluorescence intensities of GFP–VLP fell within a single peak with an average of $1.2 \pm 0.4 \times 10^4$ (Fig. 2G). In contrast to RNA pol I subunits in FCs, which showed a maximum variance of molecule numbers of about twofold, CBs were significantly more heterogeneous in their GFP–p80-coilin content (Fig. 2H). Consistent with the recent description of two distinct classes of CB based on their morphological appearance and size (Platani et al., 2000), we found two distinct peaks for the GFP–p80-coilin abundance. Small CBs of typically 200 nm in diameter contained on average 145 ± 92 GFP–p80-coilin molecules while large CBs with a diameter of up to 1 μm contained on average 1511 ± 673 molecules of GFP–p80-coilin (Fig. 2H; Table 1). Since we knew the number of GFP–p80-coilin molecules and its relative abundance compared to endogenous p80-coilin, we could estimate the absolute number of total p80-coilin molecules in small CBs to 203 ± 128 molecules and in large CBs to 2115 ± 941 molecules of p80-coilin.

To finally test whether GFP–VLP calibration could also be applied to structures outside of the cell nucleus, we probed the number of molecules of a secretory protein in exocytic and endocytic vesicles using GFP–VLP calibration. STAMP1 is a protein of the trans-Golgi network, which shuttles between the TGN and the plasma membrane and is found in exocytic and endocytic membranes (Korkmaz et al., 2002). We acquired images of cells transiently expressing GFP–STMP1, measured the total fluorescence intensity of cytoplasmic

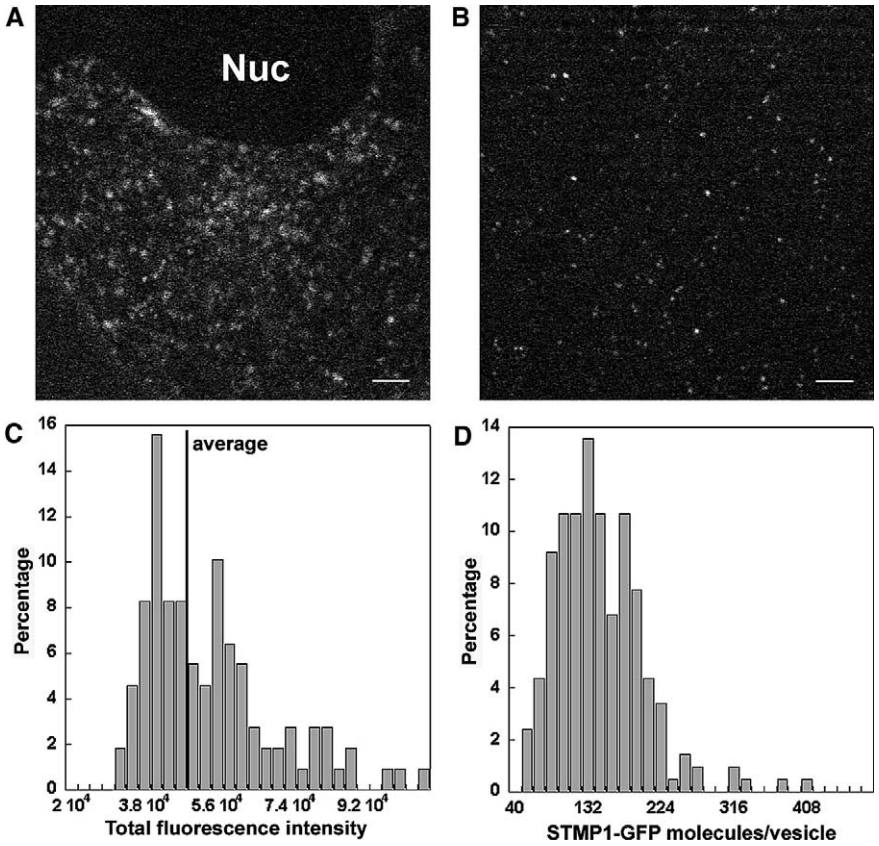

Fig. 3. Determination of the abundance of STAMP1 in exocytic vesicles. (A) The GFP-tagged STAMP1 protein was transiently expressed in CMT3 cells. GFP–STAM1 accumulated in exocytic and endocytic vesicles. (B) GFP–VLPs were visualized in the same specimen using identical imaging settings. (C) Histogram of the distribution of total fluorescence intensity of single VLP particles. (D) Histogram of the distribution of the number of GFP–STAMP1 molecules in exocytic vesicles. Bars: 2 μm.

vesicles of diameter 70–100 nm and compared it to the average intensity from GFP–VLPs imaged in the same sample using identical imaging settings (Figs. 3A and B; Table 1). We found on average 154 ± 56 GFP–STMP1 molecules in a single vesicle (Figs. 3C and D). This number is consistent with the estimate that a typical transport vesicle of diameter 70 nm can contain up to 300 transmembrane protein molecules (Hirschberg et al., 1998).

4. Discussion

We describe here a simple method for the estimation of the number of GFP-tagged molecules in a single living cell using GFP–VLP as an internal calibration standard. GFP–VLPs are ideal calibration standards since they contain a known, fixed number of fluorescent groups and GFP–VLPs have the advantage over fluorescent beads that the fluorescence signal of GFP–VLP is similar to that of many cellular structures (Figs. 2, 3). Unlike calibration methods which use a standard curve generated by a dilution series of known concentrations of recombinant GFP in solution (Hirschberg et al., 1998), VLP calibration allows observation of a standard in the same specimen as the sample of interest permitting the use of identical imaging settings and ruling out the possibility of altered fluorescence properties of the calibration standard and the test signal due to sample preparation. Although we used GFP–VLP particles located outside of cells for our experiments, GFP–VLPs can be taken up by cells (Charpilienne et al., 2001) and it should thus be possible to use them as an intracellular calibration standard. Our measurements are based on the assumption that the fluorescent properties of GFP are not dramatically different from those of GFP molecules in the extracellular VLP particles. Using two experimental systems in which the number of binding sites can be estimated independently, we demonstrate that the estimated numbers are consistent with expected values. We have applied GFP–VLP calibration to various cellular structures ranging from transcription sites and subnuclear bodies to exocytic and endocytic vesicles. Due to the spherical shape and small size of GFP–VLPs, relatively small cellular structures, such as vesicles, are ideally suited for analysis by this method. However, we find that the calibration method works equally well for thin and thick confocal optical sections and GFP–VLP calibration can thus also be used for estimation of molecule numbers in spatially more extended structures such as the MMTV array. GFP–VLP calibration is not limited to use in confocal microscopy as it worked equally well when imaging with an open or closed pinhole and we obtained similar results using either 12-bit or 16-bit imaging. It should also be possible to apply GFP–VLP calibration to deconvolution microscopy, which should allow the analysis of spatially more extended structures. In addition to its usefulness in determining the number of GFP molecules in a cell, in cases where the abundance of GFP-tagged molecules relative to an endogenous protein is known, the absolute abundance of a protein in a cellular structure or a cell can also be estimated. Using this strategy we have estimated the number of p80-coilin molecules in subnuclear Cajal bodies and we find that the abundance of p80-coilin correlates with the size of CBs, consistent with a structural role of the protein in CB formation (Tucker et al., 2001).

The main sources of error in GFP–VLP calibration are the inaccuracy in the measurements of fluorescence signals and the heterogeneity due to possible aggregation and disintegration of VLP particles. While some of the variability in the measurements is due to the inaccuracy of the fluorescence signal measurements, the fluctuations more likely reflect biological variation among cellular structures. For example, not all FCs contain the same number of genes (Junera et al., 1997) and not all MMTV arrays are similarly active (Muller et al., 2001). The fact that we easily detected two distinct, previously described populations of CBs containing distinct numbers of p80-coilin supports the accuracy of the GFP–VLP calibration method (Platani et al., 2000). Furthermore, as expected we find a significantly broader distribution of signals from GFP-fusion proteins in various biological structures compared to GFP–VLP signals, which represent a more homogenous population. Overall, we estimate the accuracy for determining the absolute number of GFP molecules by this method to be on the order of about twofold. Since we use a single average value for the GFP–VLP signal, any heterogeneity in the VLP population introduces a systematic error. We estimate this error to be about 35%, which corresponds to the typical standard deviation observed for GFP–VLP signals using 12-bit or 16-bit imaging (Figs. 1B, 2C and G, 3C). A limitation of this method is the intensity of the GFP–VLP relative to the object of interest. Since it is essential that images of sample and GFP–VLPs be acquired using identical imaging settings, objects that are very bright or very dim compared to GFP–VLPs are difficult to measure. In 12-bit imaging the average pixel intensity of GFP–VLP particles was ideally on the order of 200 intensity units after background subtraction. Since 4096 gray levels can be recorded in 12-bit imaging, the dynamic range under the conditions used here is about 20. Thus, we can estimate that a maximum of 2400 and a minimum of six fluorescent molecules can be detected in a cellular structure of similar size as GFP–VLPs. Due to limitations in detection of low signals we estimate that a more realistic lower limit of detection is on the order of 50 fluorescent molecules. Higher total numbers of GFP molecules can obviously be detected in structures of larger volume than GFP–VLPs such as the MMTV array or large CBs.

Taken together, GFP–VLP calibration is a simple method for the in vivo estimation of fluorescence signals and it should significantly facilitate the absolute quantitation of GFP proteins in single livings. The availability of information regarding absolute protein abundances should prove useful in the quantitative study of cell biological processes in living cells.

Acknowledgments

We thank A. Charpilienne for her excellent technical help in preparing VLPs, Drs. A. Lamond, M. Platani, and J. Swedlow (University of Dundee) for the GFP–p80-coilin HeLa cell line, G. Hager (NCI) for 3617 cells, and F. Saatcioglu (University of Oslo) and C. Elbi (NCI) for STAMP1–GFP. We thank Thierry Cheutin, Matthias Becker, and Jason Swedlow for critical comments. All imaging was performed in the NCI Fluorescence Imaging Facility. This work was supported in part by an "Innovation Technique et Methodologique" grant (4TM06F) from INSERM and a 5th FW grant from the European Union (QLRT 1999-00634).

References

Chalfie, M., Tu, Y., Euskirchen, G., Ward, W.W., Prasher, D.C., 1994. Green fluorescent protein as a marker for gene expression. Science 263, 802–805.

Charpilienne, A., Nejmeddine, M., Berois, M., Parez, N., Neumann, E., Hewat, E., Trugnan, G., Cohen, J., 2001. Individual rotavirus-like particles containing 120 molecules of fluorescent protein are visible in living cells. J. Biol. Chem. 276, 29361–29367.

Chiu, C.S., Kartalov, E., Unger, M., Quake, S., Lester, H.A., 2001. Single-molecule measurements calibrate green fluorescent protein surface densities on transparent beads for use with "knock-in" animals and other expression systems. J. Neurosci. Methods 105, 55–63.

Gall, J.G., 2000. Cajal bodies: the first 100 years. Annu. Rev. Cell Dev. Biol. 16, 273–300.

Gilbert, N., Lucas, L., Klein, C., Menager, M., Bonnet, N., Ploton, D., 1995. Three-dimensional co-location of RNA polymerase I and DNA during interphase and mitosis by confocal microscopy. J. Cell Sci. 108, 115–125.

Grummt, I., 1999. Regulation of mammalian ribosomal gene transcription by RNA polymerase I. Prog. Nucleic Acid Res. Mol. Biol. 62, 109–154.

Haaf, T., Hayman, D.L., Schmid, M., 1991. Quantitative determination of rDNA transcription units in vertebrate cells. Exp. Cell Res. 193, 78–86.

Hirschberg, K., Miller, C.M., Ellenberg, J., Presley, J.F., Siggia, E.D., Phair, R.D., Lippincott-Schwartz, J., 1998. Kinetic analysis of secretory protein traffic and characterization of golgi to plasma membrane transport intermediates in living cells. J. Cell Biol. 143, 1485–1503.

Jackson, D.A., Hassan, A.B., Errington, R.J., Cook, P.R., 1993. Visualization of focal sites of transcription within human nuclei. EMBO J. 12, 1059–1065.

Junera, H.R., Masson, C., Geraud, G., Suja, J., Hernandez-Verdun, D., 1997. Involvement of in situ conformation of ribosomal genes and selective distribution of upstream binding factor in rRNA transcription. Mol. Biol. Cell 8, 145–156.

Khakh, B.S., Smith, W.B., Chiu, C.S., Ju, D., Davidson, N., Lester, H.A., 2001. Activation-dependent changes in receptor distribution and dendritic morphology in hippocampalneurons expressing P2X2-green fluorescent protein receptors. Proc. Natl. Acad. Sci. USA 98, 5288–5293.

Korkmaz, K.S., Elbi, C.C., Korkmaz, C.G., Loda, M., Hager, G.L., Saatcioglu, F., 2002. Molecular cloning and characterization of STAMP1, a highly prostate specific six-trans-membrane protein that is overexpressed in prostate cancer. J. Biol. Chem. 277, 36689–36696.

Labbe, M., Baudoux, P., Charpilienne, A., Poncet, D., Cohen, J., 1994. Identification of the nucleic acid binding domain of the rotavirus VP2 protein. J. Gen. Virol. 75, 3423–3430.

Lawton, J.A., Zeng, C.Q., Mukherjee, S.K., Cohen, J., Estes, M.K., Prasad, B.V., 1997. Three-dimensional structural analysis of recombinant rotavirus-like particles with intact and amino-terminal-deleted VP2: implications for the architecture of the VP2 capsid layer. J. Virol. 71, 7353–7360.

McNally, J.G., Muller, W.G., Walker, D., Wolford, R., Hager, G.L., 2000. The glucocorticoid receptor: rapid exchange with regulatory sites in living cells. Science 287, 1262–1265.

Muller, W.G., Walker, D., Hager, G.L., McNally, J.G., 2001. Large-scale chromatin decondensation and recondensation regulated by transcription from a natural promoter. J. Cell Biol. 154, 33–48.

Olson, M.O.J., Dundr, M., Szebeni, A., 2000. The nucleolus: an old factory with unexpected capabilities. Trends Cell Biol. 10, 189–196.

O'Sullivan, A.C., Sullivan, G.J., McStay, B., 2002. UBF binding in vivo is not restricted to regulatory sequences within the vertebrate ribosomal DNA repeat. Mol. Cell Biol. 22, 657–668.

Paule, M.R., White, R.J., 2000. Survey and summary: transcription by RNA polymerases I and III. Nucleic Acids Res. 28, 1283–1298.

Phair, R.D., Misteli, T., 2001. Kinetic modelling approaches to in vivo imaging. Nat. Rev. Mol. Cell Biol. 2, 898–907.

Prasad, B.V., Wang, G.J., Clerx, J.P., Chiu, W., 1988. Three-dimensional structure of rotavirus. J. Mol. Biol. 199, 269–275.

Platani, M., Goldberg, I., Swedlow, J.R., Lamond, A.I., 2000. In vivo analysis of Cajal body movement, separation, and joining in live human cells. J. Cell Biol. 151, 1561–1574.

Stefanovsky, V.Y., Pelletier, G., Bazett-Jones, D.P., Crane-Robinson, C., Moss, T., 2001. DNA looping in the RNA polymerase I enhancesome is the result of non-cooperative in-phase bending by two UBF molecules. Nucleic Acids Res. 29, 3241–3247.

Tucker, K.E., Berciano, M.T., Jacobs, E.Y., LePage, D.F., Shpargel, K.B., Rossire, J.J., Chan, E.K.L., Lafarga, M., Conlon, R.A., Matera, A.G., 2001. Residual Cajal bodies in coilin knockout mice fail to recruit Sm snRNPs and SMN, the spinal muscular atrophy gene product. J. Cell Biol. 154, 293–308.

van Roessel, P., Brand, A.H., 2002. Imaging into the future: visualizing gene expression and protein interactions with fluorescent proteins. Nat. Cell Biol. 4, E15–E20.